CHAPTER IV

STRESS RELAXATION BEHAVIOR OF (ALA-GLY-PRO-ARG-GLY-4HYP-GLY-PLO-) GELATIN HYDROGELS UNDER ELECTRIC FIELD: TIME-ELECTRIC FIELD SUPERPOSITION

4.1 Abstract

An investigation has been conducted on stress relaxation functions and the corresponding relaxation time distribution functions of gelatin hydrogels for the effects of degree of crosslinking and the applied electric field strength. The experimental shift factors can be thus obtained from either the stress relaxation functions or the storage and loss moduli. Both approaches yield numerically the same shift factor values which successfully allow the time-electric field superposition of various related functions. The modified shift factors are obtained from the effective relaxation times and the material constant (C_r). The material constant critically depends on the degree of crosslinking and weakly on the reference electric field strength used in the superposition. The relaxation time distribution clearly indicates two modes of relaxation under an electric field. The fast mode of relaxation, which occurs only under an electric field, can be attributed to the relaxation of protons present in the gelatin hydrogels.

Keywords: Gelatin; Stress relaxation; Time–electric field superposition

4.2 Introduction

Viscoelastic properties are often used to refer to the material chemical-microstructural relationship, as viscoelastics involve both solid-state and liquid-like behaviors (Meyer *et al.*, 2009).Studies of viscoelastic materials include deformation, swelling, stability, and etc (Kunda *et al.*, 2009; Zhang *et al.*, 2008).

The present work focuses on the stress relaxation behavior, an important property for viscoelastic materials. Stress relaxation is the decrease in an internal stress when a material is held at a constant and finite strain. When an external strain is introduced to an elastic material, the applied strain causes a reversible deformation, and when the strain is removed, the residual stress rapidly relaxes to zero. Most materials are viscoelastic; when the material is subjected to an external strain, a stress is generated within the material and the generated stress relaxes through the process of stress relaxation (Matsuoka, 1992).The most simple law for the relaxation process of viscoelastic materials is described by the Maxwell model.

However, this model is not applicable towards real viscoelastic materials. Viscoelastic materials can exhibit many modes of relaxation processes. The relaxation processes can be divided into three stages: stage 1 is for the short time relaxation process (0-1 h); stage 2 is for the intermediate time relaxation (1-10^4 h); and stage 3 is for the long time relaxation process (>10^4h) (Matsuoka, 1992; Williams *et al.*, 1970).The Kohlrausch-Williams-Watts (KWW) equation is a well-known equation to describe the stage1 of the stress relaxation process (Matsuoka, 1992).

$$G(t) = G_\infty + G_o[e^{-(t/\tau)^n}] \tag{4.1}$$

where $G(t)$ is the stress relaxation function as obtained from the experiment, G_∞ is the equilibrium modulus or the long time value, t is the experimental time, τ is the effective relaxation time, and n ($0 < n \leq 1$) is the stretching parameter. Zhao *et al.* (2010) studied the stress relaxation of alginate hydrogels with covalent crosslinks; the relaxation propagated through the network connectivity. Mao *et al.* (2000)

investigated the relaxation time of gelatin hydrogels at various degrees of crosslinking. The effective relaxation time shifted to a shorter amount of time as the degree of crosslinking increased.

Furthermore, the effect of temperature on viscoelastic materials has been studied through the stress relaxation due to temperature dependent molecular rearrangement processes occurring under applied stress. The relaxation process depends on the speed of the molecular motion in which temperature (T) is varied and the resultant viscoelastic functions of viscoelastic materials can be expected to depend on temperature as well as time. Thus the relaxation function may be written as $G = G(t,T)$ (Lakes, 1998; Ferry, 1980).

If the relaxation times of all viscoelastic materials have the same temperature dependence, it is expected that it should be possible to superimpose linear viscoelastic data sets taken at different temperatures (Rubinstein *et al.*, 2003). This is commonly known as the time–temperature superposition (Tobolsky, 1956). Stress relaxation function data at any temperature (T) can be superimposed onto the data taken at a reference temperature (T_o) using a time scale shift factor (a_T) as in the following equation (Schwarzl *et al.*, 1952: Ferry, 1980).

$$a_T = \frac{\tau_i(T)}{\tau_i(T_o)} \tag{4.2}$$

where $\tau_i(T)$ and $\tau_i(T_o)$ are the characteristic time scales at T and T_o, respectively. The principle of the time-temperature superposition is based on the requirement that all time scales of the material system vary by the same factor or proportionality when temperature is varied from one to another.

There are many studies related to the time–temperature superposition in solid state materials, such as polyisobutylene (Ferry *et al.*, 1953), polybutadiene (Palade *et al.*, 1995), polyethylene (Onogi *et al.*, 1967), polyurethane (Tobolsky, 1966), and stylene-butadiene-stylene block copolymer (Fileding-Russell *et al.*, 1972). Palade *et al.* (1995) studied the time–temperature superposition and linear viscoelasticity of polybutadiene where the storage moduli and the stretching parameter depended on temperature. June *et al.* (2010) studied the temperature effect

on articular cartilage biomechanics; the stress relaxation proceeded faster and the stretching parameter decreased with increasing temperature. Chen *et al.* (2000) investigated the time–temperature superposition of amorphous ethylene–styrene inter polymers in which the shift factor decreased as a function of temperature. Le *et al.* (2003) studied the temperature dependent deformation behavior of different thermoplastic elastomers. Wortmann *et al.* (1995) investigated the stress relaxation and the time–temperature superposition of polypropylene in which the characteristic relaxation time decreased with increasing temperature. Recently, the effects of electric field on viscoelastic properties and relaxation characteristic have been studied. The time–electric field relationship was investigated by Park *et al.* (2006). It was shown that the electric field reduced the time required to obtain the saturated storage modulus value of polypropylene/layered silicate nanocomposites.

In the present work, gelatin (Ala-Gly-Pro-Arg-Gly-Glu-4Hyp-Gly-Pro-) was used as materials to investigate stress relaxation behavior. Uncrosslinked and crosslinked gelatin hydrogels were prepared by adding a glutaraldehyde solution into a gelatin solution followed by a casting method. Stress relaxation functions of the uncrosslinked and crosslinked gelatin hydrogels were measured to study the effects of electric field strength and the crosslinking ratio. The horizontal shift factors ($a_{E,exp}$) were experimentally obtained from both the stress relaxation function and the storage–loss moduli at various electric field strengths. These experimental shift factors ($a_{E,exp}$) allow the time–electric field superpositions of the moduli and the stress relaxation function to be possible. Furthermore, it will be shown that $a_{E,exp}$ can be calculated by the calculated shift factor ($a_{E,cal}$), obtained from the ratio of the effective time scales incorporated with the material constant (c_T).

4.3 Experimental

4.3.1 Materials

Gelatin powder (Type B, bovine skin, bloom strength 225, Sigma-Aldrich) which a typical structure is Ala-Gly-Pro-Arg-Gly-Glu-4Hyp-Gly-Pro, Glutaraldehyde (50 %w/v GTA solution, AR grade, Fluka) were used as the starting materials for preparing gelatin hydrogels.

4.3.2 Preparation of Gelatin Hydrogel

Uncrosslinked gelatin hydrogels were prepared via the dissolution in the 10 %v/v in deionized water at 40 °C under continuous stirring for 40 min. Crosslinked gelatin hydrogels were prepared by adding specific amount of glutaraldehyde solution into a 10 %v/v gelatin solution with the glutaraldehyde concentration varied at 3 and 7 %v/v and stir vigorously for 15 min at 40 °C to obtain homogeneous solution by magnetic stirring. Uncrosslinked and crosslinked gelatin solutions were poured into petri dishes. Hydrogels were obtained by solution casting at ambient temperature (30 °C) for 1 day and the crosslinked gelatin hydrogels were washed with deionized water 40 ml for 2 times. Finally, it was dried at room temperature to gel settle approximately at 1 mm sample thickness and 25 mm sample diameter.

4.3.3 Characterization and Testing of Uncrosslinked and Crosslinked Gelatin Hydrogels

Uncrosslinked and crosslinked gelatin hydrogels were identified for functional groups by a Fourier Transform Infrared Spectrometer (FTIR; Thermo Nicolet, Nexus 670, ATR) operated in the absorption mode with 32 scans and a resolution of ±4 cm^{-1}, covering a wavenumber range of 3500 cm^{-1} to 500 cm^{-1}, with deuteratedtriglycine sulfate as a detector.

In order to estimate the network crosslinking density, the number-average molecular weight of the polymer chain segments between two consecutive segments (M_c) was calculated using the Flory–Rehner equation (Flory and Rehner, 1943).

$$M_c = \frac{\rho V_1\left(\phi_g^{1/3} - 2\phi_g / f\right)}{\chi\phi_g^2 + \ln(1-\phi_g) + \phi_g} \tag{4.3}$$

where ρ is the density of the dry gelatin, which is studied by pycnometry, V_1 is the molar volume of the solvent, χ is the polymer–solvent interaction parameter (χ = 0.49 ± 0.05) (Flory and Rehner, 1943),and φ_g is the volume fraction of the swollen gelatin, which was estimated from the following relation:

$$\phi_s = \frac{W_0 \rho_w}{W\rho - W_0(\rho - \rho_w)} \tag{4.4}$$

where W_0 is the initial weight of the sample, W is the weight of the swollen sample, ρ_w is the density of the water at room temperature, and ρ is the density of the dry uncrosslinked gelatin films.

Electrostatic force microscopy (EFM; XE100, Park System) images were taken with a scanning electron microscope to determine the surface morphology and phase of the gelatin hydrogels, using a scan rate of 0.3 Hz, a signal amplitude of 5 V, and a scan size of 3 μm x 3 μm. Each sample was scanned at two heights above the surface. In the first scan, the probe tip responded to the van der Waals force under the tapping mode and the surface morphology was recorded. The second scan was taken under the interleave mode to detect the electric field force.

A melt rheometer (Rheometric Scientific, ARES) was used to measure the stress relaxation properties of the gelatin hydrogels. The specimens were fitted with a custom-built copper parallel plate fixture (diameter of 25 mm). A DC voltage (Instek, GFG8216A) was applied through the specimen. A digital multimeter (Tektronic Incorporation, CDM250) was used to monitor the voltage input. In these experiments, the $G(t)$ were measured as a function of time and electric field strength (0-800 V/mm). First, appropriate strains were determined for $G(t)$ to be in the linear viscoelastic regime. The suitable strain was measured to be 0.20% for both the uncrosslinked and crosslinked gelatin hydrogels. The measured stress relaxation data were then converted to the dynamic storage, loss moduli, and the relaxation time spectrum through the software program (TA Orchestrator version6.60B1, TA Instruments Incorporation).

To quantify the long-time relaxation behavior of the samples, the stress relaxation function $G(t)$ was fitted to the phenomenological KWW equation. The effective relaxation time (τ) and the stretching parameter (n) were determined by fitting stress relaxation data to equation 4.5 through a software program (Polymath version 6.10, CACHE Corporation).

Which equation 1 is replaced to determine the relaxation time distribution by an integral (Matsuoka, 1992).

$$G(t) = G_\infty + \int_0^\infty G(\tau)[e^{-(t/\tau)^n} d\tau] \quad (4.5)$$

where $G(t)$ is the stress relaxation function as obtained from the stress relaxation experiment, G_∞ is the equilibrium stress relaxation or the long time value, t is the experimental time, τ is the effective relaxation time, $G(\tau)$ is a continuous function over relaxation time, and n ($0 < n \leq 1$) is the stretching parameter. The effective relaxation time (τ) is presented on a logarithm scale. Thus, equation 4.6 can be written as:

$$G(t) = G_\infty + \int_{-\infty}^\infty H(\tau)[e^{-(t/\tau)^n} d\ln\tau] \quad (4.6)$$

where $H(\tau) = \tau G(\tau)$ is called the relaxation time distribution spectrum (Matsuoka, 1992; Fried, 2003). $H(\tau)$ was determined through the software program (TA Orchestrator version 6.60B1, TA Instruments Incorporation) using equation 4.7, where the mean relaxation time (τ_m) was determined from $H(\tau)$. The relaxation time distribution spectrum is a fundamental function of viscoelastic materials (Honerkamp *et al.*, 1993). The stretching parameter (n) can be related to the width of the relaxation time distribution spectrum (Lindsey *et al.*, 1980).

The dynamic moduli data can be obtained via a transformation of $G(t)$ in two steps. First, the stress relaxation data was converted into the relaxation time distribution spectrum, then the dynamic moduli were calculated from the relaxation time distribution spectrum by integration of the spectra as in equations 4.8 and 4.9 using the same software program (TA Orchestrator version 6.60B1, TA Instruments Incorporation) (Schwarzl, 1975).

$$G'(\omega) = G_\infty + \int_0^\infty H(\tau) \frac{\omega^2\tau^2}{1+\omega^2\tau^2} d\tau \quad (4.8)$$

$$G''(\omega) = \int_0^\infty H(\tau) \frac{\omega^2\tau^2}{1+\omega^2\tau^2} d\tau \quad (4.9)$$

where $G'(\omega)$ and $G''(\omega)$ are the dynamic storage modulus and the dynamic loss modulus as functions of frequency (ω), respectively. G_∞ is the equilibrium stress relaxation function or the long time value, $H(\tau)$ is the relaxation time distribution spectrum, τ is the integrating relaxation time, and the stretching parameter n ($0 < n \leq 1$). From $G'(\omega)$ and $G''(\omega)$ data, the relaxation time of dynamic moduli data at the crossover (τ_c) was identified at the crossover point of ($G'(\omega)$) and ($G''(\omega)$) versus frequency (ω); τ_c is reciprocal of the crossover frequency (ω_c) (Schwarzl, 1975; Belfiore, 2010; Ferry, 1980).

Horizontal shift factors of uncrosslinked and crosslinked gelatin hydrogels were determined to superimpose the G' and G'' data at different electric field strengths from 0 V/mm to 800 V/mm and identified as the experimental shift factor ($a_{E,exp}$). By definition, the shift factor due to electric field can be generally calculated and expressed as:

$$a_{E,cal} = \frac{\tau_i(E)}{\tau_i(E_o)} \quad (4.10)$$

where $\tau_i(E)$ and $\tau_i(E_o)$ are the effective relaxation time scales of equation 1 taken from the stress relaxation measurement at the electric field strengths of E and E_o, respectively (Schwarzl *et al.*, 1952; Roland *et al.*, 1992).

However, the calculated shift factors of uncrosslinked and crosslinked gelatin hydrogels as in equation4.9 do not agree numerically with the experimental shift factors as they contain an intrinsic material dependence through a constant (C_τ) which is a strong function of the material and weakly dependent on the reference electric field strength between (0 and 800 V/mm). C_τ is defined here as the ratio of $a_{E,exp}$ and $a_{E,cal}$. Therefore, the calculated shift factor of equation 9 can be modified by a constant value of C_τ as shown in the following equation 10 and can be renamed as the modified shift factor ($a_{E,mod}$).

$$a_{E,mod} = C_\tau x a_{E,cal} \quad (4.11)$$

where C_τ is the material constant which is weakly dependent on reference electric field strength, $\tau_l(E)$ and $\tau_l(E_o)$ are the effective relaxation time scales at electric field strengths of E and E_o, respectively.

4.4 Result and Discussion

4.4.1 Characterization of Uncrosslinked and Crosslinked Gelatin Hydrogels

The FTIR spectrum of uncrosslinked gelatin hydrogel shows characteristic peaks at 1250, 1550, 1630, 2922, and 3300 cm^{-1}. They correspond to the C-N stretching, the N-H bending, the C=O stretching vibration, the C-H stretching vibration, and the N-H stretching vibration, respectively. For the spectrum of the 7 %v/v crosslinked gelatin hydrogel, additional peaks appear at 1641 cm^{-1} and 1450 cm^{-1}. These peaks represent the aldimine (CH=N) stretching vibration, indicating that the crosslinking between gelatin and glutaraldehyde occurred (Nguyen *et al.*, 2010).

The glutaraldehyde crosslinking leads a significant reduction in swelling. Swelling measurements at longer times were prevented by the solubility of the hydrogel. The calculated average molecular weight between two neighboring crosslink points, M_c, decreases drastically with increasing of glutaraldehyde content, due to the formation of a packed network. The 3 %v/v and 7 %v/v crosslinked gelatin hydrogel show M_c of 1920 ± 296, and 320 ± 16 g/mol, respectively. The 7 %v/v crosslinked gelatin hydrogel possesses the lowest degree of swelling. The amount of the crosslinking agent was higher than 7 %v/v and did not induce any further change in the crosslinking density and the percentage of swelling of the crosslinked hydrogel. Fraga *et al.* (1985) reported similar results by the termination of the reaction in the thermosetting systems of gelatin films.

4.4.2 Relaxation Behavior of Uncrosslinked and Crosslinked Gelatin Hydrogels

The effects of crosslinking ratio and electric field strength on the $G(t)$, G' and G'' of the uncrosslinked and crosslinked gelatin hydrogels were investigated at electric field strengths between 0 and 800 V/mm. Fig. 4.1(a) and (b) show $G(t)$ and the shifted stress relaxation of the uncrosslinked and 7 %v/v crosslinked gelatin hydrogels in relation to time, respectively. The stress relaxation functions of the 7 %v/v crosslinked gelatin hydrogel are shown in Fig.4.1 as one of several crosslinked gelatin hydrogels investigated. Fig. 4.1(a) reveals the accelerated stress relaxation via the increases in crosslinking density and electric field. In other words, increasing molecular connectivity or increasing crosslinking ratio promotes the capability of the hydrogels to relax faster through available junctions connected with neighboring topological structures (Konyali *et al.*, 2008). On the other hand, the electric field also induces polarization and dipole-dipole interaction that effectively produce electric field-induced connectivity which in turn enhances $G(t)$. Protsenko *et al.* (2006) studied stress relaxation in porcine septal cartilage under applied electric field, they found that the specimen accelerated the relaxation of internal stress in the influence of electric field. Konyali *et al.* (2008) studied a similar effect on polyisoprene. The relaxation time of polyisoprene decreased with increasing degree of crosslinking, and the stress relaxation was rapidly distributed throughout the crosslinking molecular segments.

In Fig.4.1(b), the experimental superimpositions of the stress relaxations ($G(t)$-$t/a_{E,exp}$) of the uncrosslinked and 7 %v/v crosslinked gelatin hydrogels are shown to produce master curves through the horizontal shifting of the stress relaxations at various electric field strengths towards the stress relaxation functions at the reference electric field (0 V/mm). The superimpositions of these $G(t)$-$t/a_{E,exp}$ functions obviously produce two distinct superimposed master curves, one for the uncrosslinked and one for the 7 %v/v crosslinked gelatin hydrogels. The experimental shift factors ($a_{E,exp}$) of the uncrosslinked gelatin hydrogel at various electric field strengths (50, 100, 200, 400, and 800 V/mm) are 0.40, 0.36, 0.30, 0.23, and 0.16, respectively. While the value of $a_{E,exp}$ of the 7 %v/v crosslinked gelatin hydrogel are 0.92, 0.85, 0.70, 0.65, and 0.55. Effective relaxation times (τ) of the

uncrosslinked and 7 %v/v crosslinked gelatin hydrogels, obtained from fitting stress relaxation data with KWW equation 4.1, both decrease with increasing electric field strength, apparently due to the increase in the molecular connectivity under the applied electric field, as shown in Table 4.1. Park *et al.* (2006) reported a similar effect of electric field strength on a time scale to reach equilibrium property of polypropylene nanocomposites. The electric field reduced the characteristic time of the polypropylene nanocomposites. Le *et al.* (2003) found that the shift factor at different temperatures of polypropylene and nitrile rubber decreased with increasing network structure density.

Fig.4.2(a) and (b) show the storage modulus (G') and experimentally shifted storage modulus vs. frequency (rad/s), where the G' of the uncrosslinked and crosslinked gelatin hydrogels were obtained from the transformation of $G(t)$ using equations 4.7 and 4.8 and the software program (TA Instruments Incorporation, TA Orchestrator version 6.60B1). In Fig. 4.2(a), G' of the gelatin hydrogels increases with increasing of frequency (rad/s) until reaching plateaus at high frequencies, a typical behavior of a gelatin structure (Protsenko *et al.*, 2006). Shiga *et al.* (1993) found that G' increased gradually with frequency, whether an electric field was applied or not. Puvanatvattana *et al.* (2008) reported that for the poly(3-thiophene acetic acid)/polyisoprene suspension G' increased with increasing frequency indicative of solid-like behavior. Wichiansee and Sirivat (2009) reported a similar feature for the poly(dimethylsiloxane) and poly(3,4-ethylenedioxythiophene)/poly(stylene sulfonic acid)/ethylene glycol blends. For both uncrosslinked and crosslinked gelatin hydrogels, the G' at the electric field strength of 800 V/mm are higher than those of the electric field strength of 0 V/mm. As an electric field is applied, the gelatin structure responds by generating induced dipole moments, leading to intermolecular interactions and thus higher chain rigidity, as indicated by the resultant higher G' values (Wichiansee and Sirivat, 2009).

In Fig. 4.2(b), the $a_{E,exp}$ used for the shifting of the storage modulus (G'-$\omega a_{E,exp}$ function) of these hydrogels are the same experimental shift factors used for the shifting of $G(t)$ as in Fig.4.1(b).

Fig.4.3(a) shows G'' of the uncrosslinked and 7 %v/v crosslinked gelatin hydrogels in relation to frequency. The G'' of the uncrosslinked and 7 %v/v

crosslinked gelatin hydrogels also increase with increasing crosslinking ratio and applied electric field strength, apparently due to the higher induced intermolecular interaction (Hao, 2005). Tangboriboon *et al.* (2009) found that the G'' of lead zirconatetitanate/acrylic elastromer composites increased with electric field strength due to the effect of piezoelectric particles acting as a reinforcing filler. The time-electric field superimposition of the loss modulus (G''-$\omega a_{E,exp}$ function) of the uncrosslinked and 7 %v/v crosslinked gelatin hydrogels are shown in Fig.4.3(b). The same experimental shift factors for the shifting of $G(t)$ and the shifting of G' are used here resulting in two separate G''-$\omega a_{E,exp}$ functions.

Table 4.1 summarizes the relaxation times (τ) and the stretching parameter (n) of the uncrosslinked and crosslinked gelatin hydrogels as obtained by three different methods: τ from KWW; τ_c from the dynamic crossover between G' and G''; and τ_m from the relaxation time distribution spectrum. From these methods, the relaxation times of all gelatin hydrogels decrease with increasing electric field strength and crosslinking density, reaffirming the more rapid relaxation rate. The stretching parameter (n) is related to the width of the relaxation time distribution spectrum (Honerkamp *et al.*, 1993; Lindsey *et al.*, 1980), in that n increases with increasing electric field strength and degree of crosslinking.

Fig.4.4 shows the experimental shift factors ($a_{E,exp}$) and the modified shift factors ($a_{E,mod}$) obtained from the effective relaxation times (equation 1) with C_τ according to equation 4.11, of the uncrosslinked and crosslinked gelatin hydrogels at various electric field strengths (50, 100, 200, 400, and 800 V/mm), at the reference electric field strength of 0 V/mm. Both shift factors of the uncrosslinked, 3 %v/v crosslinked, and 7 %v/v crosslinked gelatin hydrogels decrease with increasing electric field strength. The modified shift factors, as obtained from the adjustment of effective relaxation times with a material constant (C_τ); the chosen values are tabulated in Table 4.2. It can be concluded that the material constant is apparently dependent on the crosslinking density and weakly dependent on the reference electric field strength.

4.4.2 Effect of Degree of Crosslinking and Electric Field Strength on Relaxation Time Distribution Spectrum

Superimposition of relaxation time distributions of the uncrosslinked, 3 %v/v crosslinked, and 7 %v/v crosslinked gelatin hydrogels are shown in Fig.4.5. From the distributions, the means of the relaxation time distributions (τ_m) can be calculated and they are tabulated in Table 4.1. The τ_m shifts towards the smaller values with increasing degree of crosslinking and electric field strength. In addition, the width of relaxation time distribution also decreases with increasing degrees of crosslinking and electric field strength, as the relaxation time and the width of relaxation time distribution corresponds with the elasticity of materials and the network connectivity of these hydrogels (Honerkamp *et al.*, 1993).

It may be noticed that the relaxation time distributions of the hydrogels are single peaked when the electric field is off. However, when the electric field is on, they become double peaked consisting of a fast relaxation mode and the slow relaxation mode, the latter always appears whether the electric field is on or off. The appearance of fast relaxation mode is related to a water proton ion present in the hydrogel while the slow relaxation mode responses to the structural relaxation of the hydrogel.

The experimental shift factors ($a_{E,exp}$) are applied to superimpose the relaxation time distributions of the hydrogels. In summary, the same a_E, in response to various electric field strengths, are successfully used in the shifting of the $G'(\omega)$, $G''(\omega)$, $G(t)$, and $H(\tau)$ functions.

The relaxation times of a water proton ion in the uncrosslinked gelatin hydrogel are 1.14, 0.95, 0.97, 0.98, and 0.94 s at 50, 100, 200, 400, and 800V/mm, respectively. The relaxation times of a water proton ion in the 3 %v/v crosslinked gelatin hydrogel are 0.89, 0.95, 0.88, 0.81, and 0.77 s at 50, 100, 200, 400, and 800V/mm, respectively. The relaxation times of a water proton ion in the 7 %v/v crosslinked gelatin hydrogel are 0.83, 0.87, 0.87, 0.84, and 0.71s at 50, 100, 200, 400, and 800V/mm, respectively. The relaxation times of water protons fall in the range of 0.71 to 1.14 s. Martron *et al.* (1980) studied the relaxation time of a water proton, and they found the relaxation time of water protons was between 0.53 to 1.87 s. Thus it appears that the fast relaxation mode is due to the protonation of

water molecules resulting proton ions in the hydrogels. Chatterjee and Bohidar (2005) studied the effect of cations on properties of gelatin hydrogels in which the calcium ion (Ca^{2+}), sodium ion (Na^{+}), and potassium ion (K^{+}) were bound to the carboxyl groups of the amino acid on the backbone of the gelatin structure. Moreover the fast mode relaxation time was shifted to shorter time scales as the charge density and salt concentration were increased. However, the slow relaxation mode was less sensitive in additional salt concentration (Chatterjee and Bohidar, 2005). Richard (1898) reported that the hydrogen ion (H^{+}) was bounded to the carboxyl group of gelatin.

Loeb *et al.* (1964) studied the hydrogen ion binding to ribonuclease, where the carboxyl group was able to bind with the hydrogen ion. It has been known that the protons generated are capable of binding themselves with the carboxyl group of the gelatin structure (Chatterjee and Bohidar, 2005; Richard, 1898), in which the decomposition of water molecules can be confirmed by the EFM phase measurement as shown in Fig. 4.6(a) and (b). Figure 4.6(a) shows the topological surface of a gelatin hydrogel; it is far from being smooth at a nano scale. Figure 4.6(b) shows the phase image of the same gelatin hydrogel. The image exhibits the charge distribution within the gelatin hydrogel; the light areas indicate the presence of the protons in which proton ion charge distribution in our materials are weakly bound with gelatin chain structure so water proton ion is not effectively with the slow relaxation mode. Mao *et al.* (2000) studied the relaxation time distribution function of a gellan hydrogel in which the characteristic τ_m moved to a shorter time scale as Ca^{2+} concentration increased. Chatterjee and Bohidar (2005) found that the $H(\tau)$ of a gelatin hydrogel exhibited two distinct peaks with increases in the Ca^{2+}, Na^{+}, and K^{+} concentrations.

4.5 Conclusions

The relaxations of uncrosslinked and crosslinked gelatin hydrogels have been investigated under the effects of the degree of crosslinking and electric field strength. The characteristic relaxation time can be estimated by three methods; KWW; the dynamic crossover; and the relaxation time distribution spectrum $H(\tau)$.

For the uncrosslinked, 3 %v/v crosslinked and 7 %v/v crosslinked gelatin hydrogels, the relaxation times decrease with increasing degrees of crosslinking and the applied electric field strengths. This is due to the increase in the molecular connectivity that promotes the capability of the stress relaxation process. The stress relaxation process of the uncrosslinked and crosslinked gelatin hydrogels shows two relaxation time modes under an applied electric field: fast relaxation mode and slow relaxation mode. The experimental shift factors ($a_{E,exp}$) of the uncrosslinked, 3 %v/v crosslinked, and 7 %v/v crosslinked gelatin hydrogels decrease with increasing electric field strength. The $a_{E,exp}$ characteristic is analogous to the time-temperature superposition. Thus, the existence of the time-electric field superposition is demonstrated here. Furthermore, $a_{E,exp}$ can be used on the shifting of $G'(\omega)$-$G''(\omega)$-$G(t)$-$H(\tau)$ functions. Effective relaxation times from stress relaxation experiment are used to determine the calculated shift factor, $a_{E,cal}$. The correlation between $a_{E,exp}$ and $a_{E,cal}$ is found to be dependent of the material constant and independent of the applied electric field.

4.6 Acknowledgements

The authors are gratefullyacknowledged the financial supports from the Conductive and Electroactive Polymers Research Unit of Chulalongkorn University; the Thailand Research Fund (TRF-RTA and MRG 5380100); the Royal Thai Governmentandthe Doctoral Scholarship from the Thailand Graduate Institute of Science and Technology (TGIST) (TG-33-09-53-003D).

4.7 References

Belfiore, L.A. (2010) Physical Properties of Macromolecules. New Jersey: John Wiley.

Chatterjee, S. and Bohidar, H.B. (2005) Effect of cationic size on gelation temperature and properties of gelatin hydrogels. International Journal of Biological Macromolecules, 35, 81-88.

Chen, H.Y., Stepanov, E.V., Chum, S.P., Hiltner, A., and Bear, E. (2000) Linear stress relaxation behavior of amorphous ethylene-styrene interpolymers. Macromolecules, 33, 8870-8877.

Ferry, J.D. (1980) Viscoelastic Properties of Polymers, 3rd ed. New York: John Wiley.

Ferry, J.D., Grandine, L.D., and Fitzgerald, E.R. (1953) The relaxation distribution function of polyisobutylene in the transition from rubber-like to glass-like behavior. Journal of Applied Physics, 24, 911.

Fielding-Russell, G.S. and Fitzhugh, R.L. (1972) Time-temperature superposition of a styrene-butadiene-styrene block copolymer cast from organic solvents. Journal of Polymer Science Part A-2: Polymer Physics, 10, 1625-1629.

Flory, P.J. and Rehner, J. (1943) Statistical mechanics of cross-linked polymer networks II.Swelling. Journal of Chemical Physics, 11, 521-526.

Fraga, A.N. and Williams, R.J.J. (1985) Thermal properties of gelatin films. Polymer, 26, 113-118.

Fried, J.R. (2003) Polymer Science and Technology, 2nd ed. Englewood Cliffs: Prentice Hall.

Hao, T. (2005) Electrorheological Fluids the Non-aqueous Suspensions, Amsterdam: Elsevier.

Honerkamp, J. and Weese, J. (1993) A nonlinear regularization method for the calculation of relazation spectra. Rheologica Acta, 32, 65-73.

June, R.K. and Fyhrie, D.P. (2010) Temperature effects in articular cartilage biomechanics. The Journal of Experimental Biology, 13:3934-3940.

Konyali, H., Menceloglu, Y., and Erman, B. (2008) Long time stress relaxation of amorphous networks under uniaxial tension: The dynamic constrained junction model. Polymer, 49, 1056-1065.

Kundu, S. and Crosby, A.J. (2009) Cavitation and fracture behavior of polyacrylamide hydrogel. Soft Materials, 5, 3963-3968.

Lakes, R.S. (1998) Viscoelastic Solids. Washington, D.C: CRC Press.

Larson, R.G. (1999) The Structure and Rheology of Complex Fluids. New York: Oxford University Press.

Le, H.H., Lupke, T., Pham, T., and Radusch, H.J. (2003) Time dependent deformation behavior of thermoplastic elastromers. Polymer, 44, 4589-4597.

Lindsey, C.P. and Patterson, G.D. (1980) Detailed comparison of the Williams-watts and Cole-davidson functions. Journal of Chemical Physics, 73, 3348.

Loeb, G.I. and Saroff, H.A. (1964) Chloride- and hydrogen-ion binding to ribonuclease. Biochemistry, 13, 1819-1826.

Mao, R., Tang, J., and Swanson, B.G. (2000) Relaxation time spectrum of hydrogels by contin analysis. Journal of Food Science, 65, 374-381.

Marton, A., Elvidge, J.A., and Inczedy, J. (1980) Measurement of the stress relaxation time of water proton ion in ion exchanger-water systems. Journal of Chromatography A, 201, 79-84.

Matsuoka, S. (1992) Relaxation Phenomena in Polymers. New York: Cambridge University Press.

Mayer, M. and Chawla, K.K. (2009) Mechanical Behavior of Materials. New York: Cambridge University Press.

Nguyen, T.H. and Lee, B.T. (2010) Fabrication and characterization of cross-linked gelatin electro-spun nano-fibers. Journal of Biomedical Science and Engineering, 3, 1117-1124.

Onogi, S., Asada, T., Fukui, Y., Fujisawa, T. (1967) Time-temperature superposition of time-dependent birefringence for low-dendity polyethylene. Journal of Polymer Science Part A-2: Polymer Physics, 5, 1067-1078.

Palade, L.L., Verney, V., and Attane, P. (1995) Time-temperature superposition and linear viscoelasticity of polybutadienes. Macromolecules, 28, 7051-7057.

Park, J.U., Choi, Y.S., Cho, K.S., Kim, D.H., Ahn, K.H., and Lee, S.J. (2006) Time-electric field superposition in electrically activated polypropylene/layered silicate nanocomposites. Polymer, 47, 5145-5153.

Protsenko, D.S., Ho, K., and Wong, B.J.F. (2006) Stress relaxation in porcine septal cartilage during electromechanical reshaping: Mechanical and electrical responses. Annals of Biomedical Engineering, 34, 455-464.

Puvanatvattana, T., Chotpattananont, D., Hiamtup, P., Niamlang, S., Kunanuruksapong, R., Sirivat, A., and Jamieson, A.M. (2008) Electric field induced stress moduli of polythiophene/polyisoprene suspensions: Effects of particle conductivity and concentration. Materials Science and Engineering: C, 28, 119-128.

Richards, T.W. (1898) The relation of the taste of acids to their degree of dissociation. Journal of the American Chemical Society, 20, 121-126.

Roland, C.M. and Ngai, K.L. (1992) Segmental relaxation and correlation of time and temperature dependencies in poly(vinyl methyl ether)/polystyrene mixtures. Macromolecules, 25, 363-367.

Rubinstein, M. and Colby, R.H. (2003) Polymer Physics. New York: Oxford University Press.

Schwarzl, F. and Staverman, A.J. (1952) Time-temperature dependence of linear viscoelastic behavior. Journal of Applied Physics, 23, 838-843.

Schwarzl, F.R. (1975) Numerical calculation of stress relaxation modulus from dynamic data for linear viscoelastic materials. Rheologica Acta, 14, 581-590.

Shiga, T., Ohta, T., Hirose, Y., Okada, A., and Kurauchi, T. (1993) Electroviscoelastic effect of polymeric composites consisting of polyelectrolyte particles and polymer gel. Journal of Materials Science, 28, 1293-1299.

Tangboriboon, N., Sirivat, A., Kunanuruksapong, R., and Wongkasemjit, S. (2009) Electrorheological properties *of* novel piezoelectric lead zirconate titanate Pb(Zr0.5,Ti0.5)O3-acrylic rubber composites. Materials Science and Engineering: C, 29, 1913-1918.

Tobolsky, A.V. (1956) Stress relaxation studies of the viscoelastic properties of polymers. Journal of Applied Physics, 27, 673-685.

Tobolsky, A.V. (1966) Properties of linear elastomeric polyurethane. Journal of Applied Polymer Science, 10, 1837-1844.

Tungkavet, T., Pattavarakorn, D., and Sirivat, A. (2012) Bio-compatible gelatins (Ala-Gly-Pro-Arg-Glu-4Hyp-Gly-Pro-) and electromechanical properties: effects of temperature and electric field. Journal of Polymer Research, 19, 9759.

Wichiansee, W. and Sirivat, A. (2009) Electrorheological properties of poly(dimethylsiloxane) and poly(3,4-ethylenedioxy thiophene)/poly(styrene sulfonic acid)/ethylene glycol blends, Materials Science and Engineering: C, 29, 78-84.

Williams, G. and Watts, D.C. (1970) Non-symetrical dielectric relaxation behavior arising from a simple empirical decay function. Transactions of Faraday Society, 66, 80-85.

Wortmann, F.J. and Schulz, K.V. (1995) Stress relaxation and time/temperature superposition of polypropylene fibres. Polymer, 36, 315-321.

Zhang, Y., Matsumoto, E.A., Peter, A., Lin, P.C., Kamien, R.D., and Yang, S. (2008) One-step nanoscale assembly of complex structures via harnessing of an elastic instability. Nano Letter, 8, 1192-1196.

Zhao, X., Huebsch, N., Mooney, D.J., and Suo, Z. (2010) Stress-relaxation behavior in gels with ionic and covalent crosslinks. Journal of Applied Physic, 107, 063509–5.

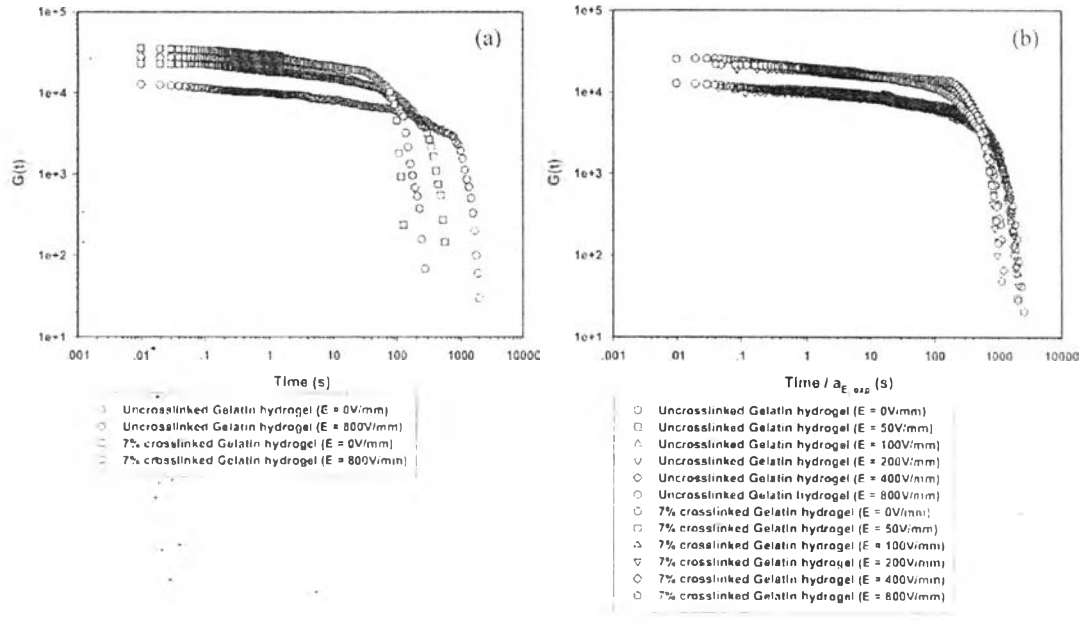

Figure 4.1 (a) Stress relaxations of uncrosslinked and 7 %v/v crosslinked gelatin hydrogels at 0 and 800 V/mm and (b) stress relaxation master curves of uncrosslinked and 7 %v/v crosslinked gelatin hydrogels at electric field strengths between 0 and 800 V/mm (sample diameter 25 mm, gel thickness 0.988 mm, 25 °C, 0.20 %strain).

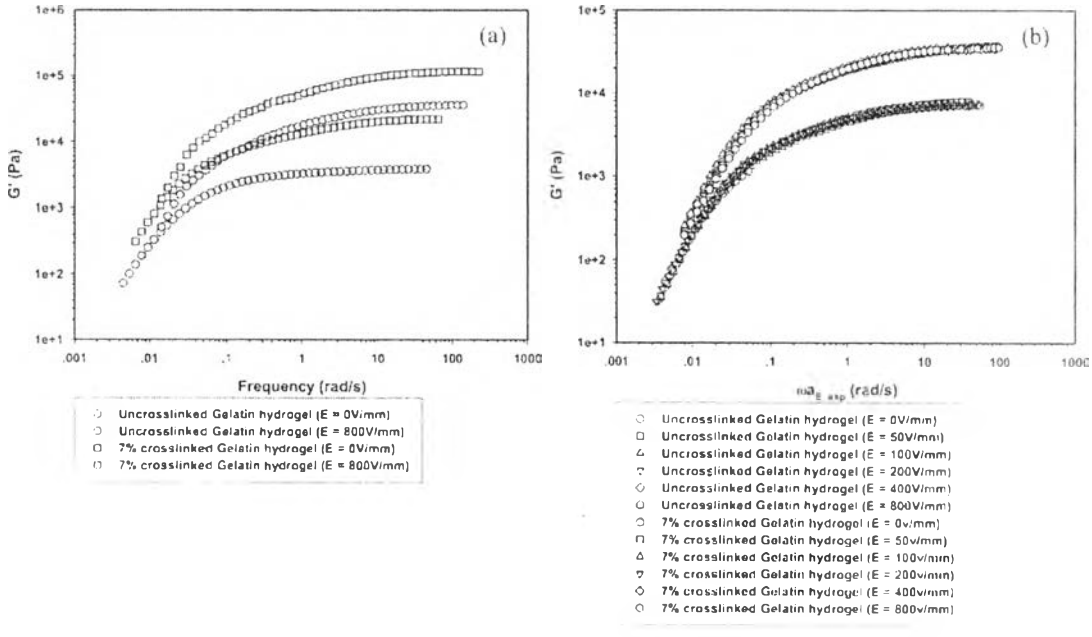

Figure 4.2 (a) Storage modulus of uncrosslinked and 7 %v/v crosslinked gelatin hydrogels at 0 and 800 V/mm and (b) storage modulus master curves of uncrosslinked and 7 %v/v crosslinked gelatin hydrogels at electric field strengths between 0 and 800 V/mm (sample diameter 25 mm, gel thickness 0.988 mm, 25 °C, 0.20 %strain).

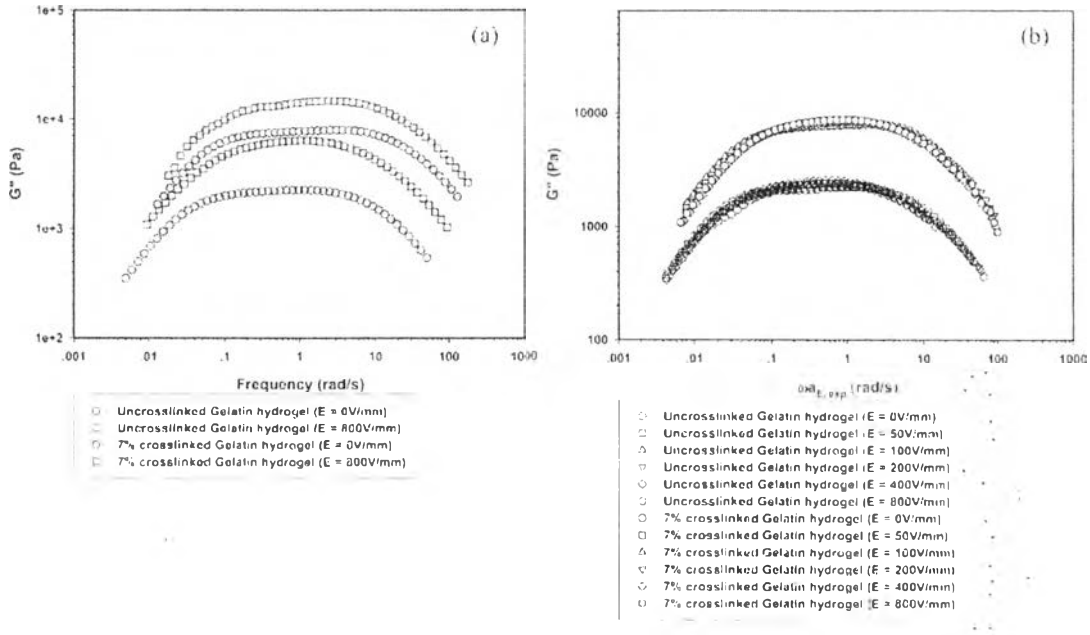

Figure 4.3 (a) Loss modulus of uncrosslinked and 7 %v/v crosslinked gelatin hydrogels at 0 and 800 V/mm and (b) loss modulus master curves of uncrosslinked and 7 %v/v crosslinked gelatin hydrogels at electric field strength varied between 0 and 800 V/mm (sample diameter 25 mm. gel thickness 0.988 mm, 25 °C, 0.20 %strain).

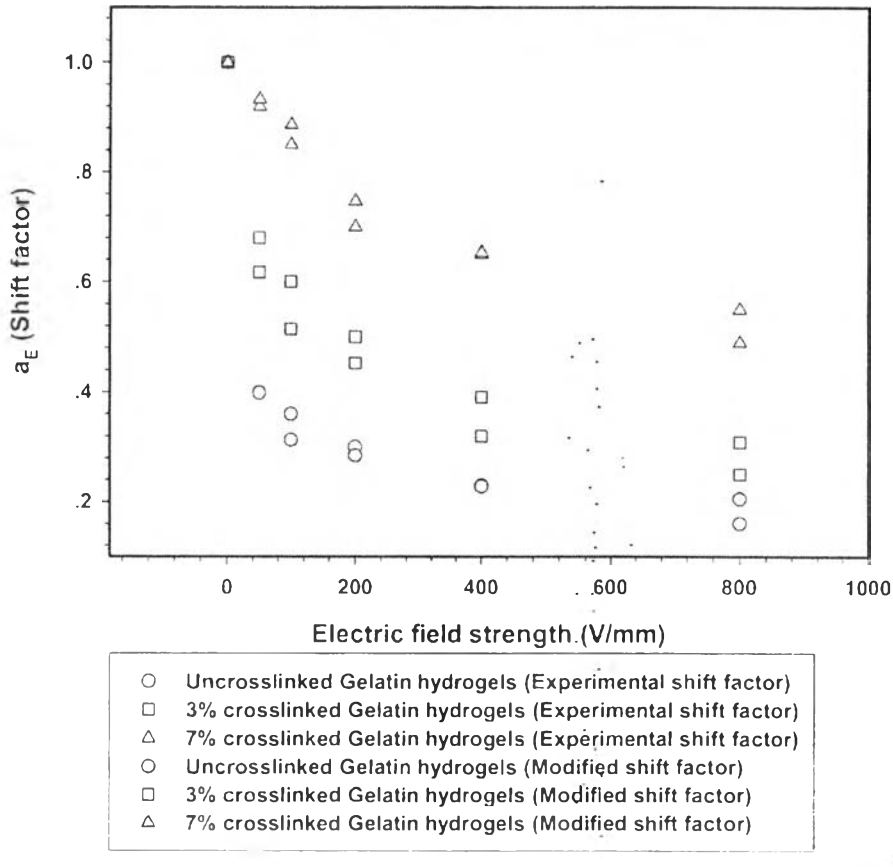

Figure 4.4 The experimental and modified shift factors of uncrosslinked, 3 %v/v crosslinked and 7 %v/v crosslinked gelatin hydrogels vs. electric field at the reference electric field of 0 V/mm (sample diameter 25 mm, gel thickness 0.988 mm, 25 °C, 0.20 %strain).

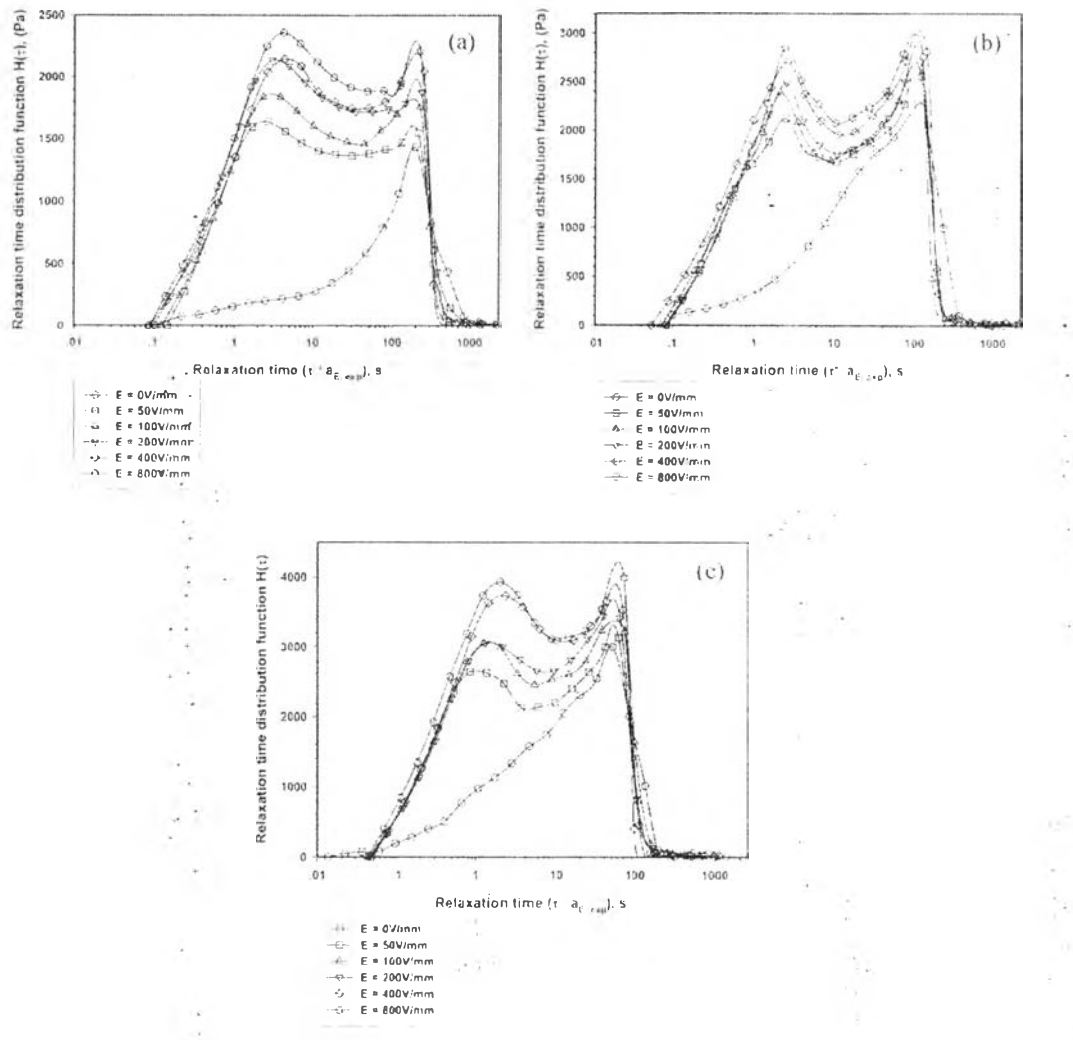

Figure 4.5 Superimpositions of the relaxation time distribution functions $H(\tau)$ of the gelatin hydrogels at various electric field strengths: (a) uncrosslinked gelatin hydrogels; (b) 3 %v/v crosslinked gelatin hydrogels and; (c) 7%v/v crosslinked gelatin hydrogels (0.20 %strain, 25 °C, samples = 5).

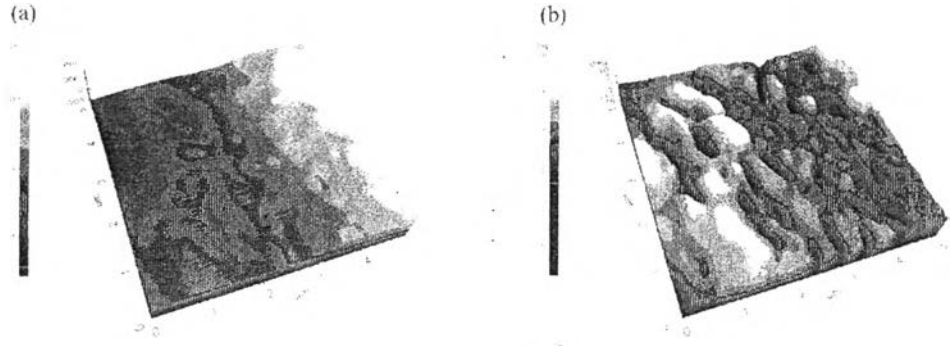

Figure 4.6(a) Topology image of uncrosslinked gelatin hydrogel and (b) EFM image under 5V of voltage bias of uncrosslinked gelatin hydrogel at 300K.

Table 4.1 Relaxation parameters of uncrosslinked, 3 %v/v crosslinked and 7 %v/v crosslinked gelatin hydrogels at various electric field strengths, at 25 °C and 0.20 %strain

Materials	E (V/mm)	Storage modulus crossover (G'_c) (Pa)	Time scale at dynamic crossover (τ_c)(s)	Effective relaxation time (τ)(s)	n ($0<n<1$)	R^2	Mean relaxation time from relaxation distribution functions (τ_m)(S)
	0	2596 ± 166	160 ± 28	154 ± 44	0.284 ± 0.02	0.977	196
	50	3671 ± 170	90 ± 10	70 ± 15	0.373 ± 0.02	0.983	74
Uncrosslinked	100	4615 ± 196	68 ± 7	55 ± 10	0.399 ± 0.02	0.988	62
gelatin hydrogel	200	5249 ± 194	54 ± 5	50 ± 8	0.419 ± 0.03	0.982	54
	400	6917 ± 179	45 ± 4	40 ± 5	0.464 ± 0.05	0.985	45
	800	8667 ± 165	38 ± 4	36 ± 4	0.475 ± 0.03	0.988	34
	0	3813 ± 213	103 ± 21	123 ± 40	0.310 ± 0.02	0.968	128
	50	4682 ± 228	68 ± 7	60 ± 15	0.439 ± 0.02	0.981	63
3% Crosslinked	100	5685 ± 202	60 ± 6	50 ± 10	0.483 ± 0.02	0.983	53
gelatin hydrogel	200	7840 ± 374	43 ± 4	44 ± 8	0.507 ± 0.02	0.984	42
	400	10975 ± 310	41 ± 3	38 ± 6	0.510 ± 0.03	0.984	37
	800	11849 ± 309	34 ± 4	30 ± 5	0.545 ± 0.03	0.984	28
	0	4574 ± 233	60 ± 8	57 ± 22	0.437 ± 0.05	0.975	51
	50	5418 ± 236	50 ± 6	40 ± 18	0.449 ± 0.02	0.989	45
7% Crosslinked	100	8169 ± 164	45 ± 4	38 ± 10	0.495 ± 0.05	0.979	40
gelatin hydrogel	200	8282 ± 196	39 ± 4	32 ± 6	0.537 ± 0.02	0.974	32
	400	12207 ± 295	31 ± 3	28 ± 6	0.588 + 0.04	0.979	30
	800	14881 ± 252	26 ± 3	21 ± 4	0.622 ± 0.04	0.974	25

Table 4.2 Material constants (C_r) of uncrosslinked, 3 %v/v crosslinked and 7 %v/v crosslinked gelatin hydrogels at various reference electric field strengths (V/mm)

Material constants	**Reference electric field strength (V/mm)**					
(C_r) of hydrogels	0	50	100	200	400	800
Uncrosslinked gelatin hydrogels	0.88	0.85	0.80	0.78	0.73	0.70
3 % crosslinked gelatin hydrogels	1.26	1.03	0.95	0.93	0.90	0.88
7 % crosslinked gelatin hydrogels	1.33	1.20	1.19	1.19	1.18	1.14